ELSEVIER

Journal of Electroanalytical Chemistry 397 (1995) 271–278

JOURNAL OF ELECTROANALYTICAL CHEMISTRY

Particle size effects for oxygen reduction on dispersed silver + carbon electrodes in alkaline solution

Yifu Yang [*,a,1], Yunhong Zhou [b]

[a] *Zhuhai Institute of New Technology, Zhuhai 519015, People's Republic of China*
[b] *Department of Chemistry, Wuhan University, Wuhan 430072, People's Republic of China*

Received 9 May 1995

Abstract

Ag + C electrocatalysts with different Ag particle-size distributions were prepared by functional ion preadsorption method. The effects of the preadsorption of different halogen ions on carbon on Ag particle size and crystal structure were studied by transmission electron microscopy and a selected area diffraction method. The adsorption characteristics of Ag^+ on activated carbon were measured by an argentimetry method. The catalytic behaviour of Ag + C catalysts with different Ag particle size distributions for oxygen reduction in KOH solution was investigated using a soft-embedded microelectrode and a soft-embedded rotating disc electrode with a platinum ring electrode. The results showed that oxygen reduction was a structure-sensitive reaction on silver particles. Decreased Ag particle size has a complicated effect on the four-electron reduction, but a favourable effect on two-electron reduction.

Keywords: Electrode material; Electrocatalyst; Oxygen reduction; Silver + carbon

1. Introduction

Oxygen electrocatalysis is of special importance to many electrochemical processes. The kinetics and mechanisms of oxygen reduction have been investigated for a wide range of cathode materials and electrolytes. Generally, they are functions of many experimental factors, as well as the electrode materials.

The reduction of oxygen in alkaline electrolytes can proceed by two overall pathways [1]: the direct four-electron pathway

$$O_2 + 2H_2O + 4e^- \rightarrow 4OH^- \quad \text{(I)}$$

and the peroxide pathway

$$O_2 + H_2O + 2e^- \rightarrow HO_2^- + OH^- \quad \text{(II)}$$

Reaction (II) can be further followed by either the reduction of peroxide

$$HO_2^- + H_2O + 2e^- \rightarrow 3OH^- \quad \text{(III)}$$

or the decomposition of peroxide

$$2HO_2^- \rightarrow 2OH^- + O_2 \quad \text{(IV)}$$

Silver has a reasonably high catalytic activity for oxygen reduction in alkaline electrolyte. Furthermore, it is a good catalyst for perhydroxyl ion decomposition [2,3]. For this reason, silver has been considered as a potential oxygen reduction catalyst in fuel cells [4] and metal|air batteries [5].

Numerous studies [6–12] have been reported on the kinetics of oxygen reduction on a bulk silver electrode. The literature data with respect to the kinetic parameters, the suggested reaction paths and mechanisms for this reaction seem to vary considerably. It was assumed that this was due to different pretreatments of the silver electrode, which resulted in differences in the nature of the electrode surface.

For the optimum utilization of silver, it should be dispersed as small particles on a conductive support such as high surface area carbon powder. As a result, the metal particle size effect for oxygen reduction becomes extremely important.

The metal particle size effect is very complicated. At least six aspects should be considered when changing metal particle size: (i) the change in geometric parameters

* Corresponding author.
[1] Present address: Electrochemistry Group, Department of Chemistry, University of Southampton, Highfield, Southampton SO17 1BJ, e-mail: yy@soton.ac.uk.

SSDI 0022-0728(95)04178-8

such as crystal structure, interatomic distance, grain size, structural irregularities (defects, kinks, dislocations); (ii) the change in electronic parameters (e.g. work function, percentage d character, d-band vacancy); (iii) the change in the active sites; (iv) the change in kinetic parameters; (v) the change in the adsorption properties of reactants/intermediates (bond strength, coverage); (vi) the interaction between metal and support. Normally, these changes are not independent; there are some correlations among them.

Platinum particle size effects for oxygen reduction have been widely investigated, but to our knowledge no data about the effects of Ag particle size on oxygen reduction have been reported. This is partially due to the difficulty in preparing Ag + C catalyst series with different Ag particle size distribution.

In a recent paper [13], we introduced a new method — the functional ion preadsorpton method — for the preparation of a highly dispersed metal + support catalyst. In the present work, this method was utilized to prepare several Ag + C catalysts with different Ag particle size dispersions. The effects of Ag particle size on oxygen reduction were investigated by transmission electron microscopy and by soft-embedded microelectrode and rotating-disc electrode methods.

2. Experimental

2.1. Catalyst preparation

Ag + C catalyst was prepared by the functional ion preadsorption method using analytical grade $AgNO_3$ (Koch-Light Ltd., Haverhill, Suffolk, UK) and activated carbon (Darco KB, Aldrich Chemicals, Gillingham, UK). The surface area of the carbon was 1500 $m^2\ g^{-1}$ (dry base) and the pore volume was 1.5 $cm^3\ g^{-1}$ (dry base). The carbon powder was dried at 80°C for 72 h before use. Cl^-, Br^- and I^- were selected as functional ions for preadsorption on carbon. Analytical grade NaCl, KBr and NaI (BDH Chemicals, Poole, UK) were used to prepare halide solutions. The concentrations of the halide solutions were 0.01 M, and the concentration of the $AgNO_3$ solution was 50 mg Ag l^{-1}.

First, carbon powder was impregnated with halide solution for 10 h (in a thermostat bath with stirring) for preadsorption of halogen ions. The supernatant was separated by centrifugation. Then a certain amount of $AgNO_3$ solution was added to the reaction bath so that it has the desired metal loading. After the Ag^+ ion had been precipitated with the halogen ion on the carbon surface for a few hours, enough $N_2H_4 \cdot H_2O$ solution was added in to reduce the Ag(+). The sample was washed with distilled water several times, dried at 80°C for 3 h and ground in an agate mortar. The main conditions for sample preparation are listed in Table 1.

All solutions used in this work were prepared with double-distilled water.

2.2. Adsorptive capacity measurement

To analyse the effect of halogen ion preadsorption on Ag particle size distribution, the adsorption equilibrium curve of Ag^+ on Darco KB was measured. Briefly, the procedure was as follows: after Ag^+ adsorption equilibrium has been achieved, the supernatant was separated. The concentration of Ag^+ in the supernatant was measured using the argentimetry method [14] (Volhard's method).

2.3. Transmission electron microscopy

Specimens for transmission electron microscopy (TEM) were prepared in the same way as that described elsewhere [13]. An H-7000 transmission electron microscope (Hitachi Ltd., Tokyo, Japan) was used to analyse the Ag particle size distribution. The Ag particle crystal structure and orientation were analysed with the selected area diffraction (SAD) mode of TEM. The electron beam accelerating voltage was 100 kV and the corresponding electron wavelength was $\lambda = 0.0037$ nm. The purity of Ag particles was analysed by the energy dispersive spectrum (EDS) method.

2.4. Electrochemical measurement

Soft-embedded microelectrode

A soft-embedded microelectrode (SE-ME), which is very useful for studying powder catalysts, was used as the working electrode for the measurement of the polarization curve of oxygen reduction on a Ag + Darco KB catalyst. The diameter of the microelectrode was 30 μm. The method for making SE-ME was given in Ref. [13]. A saturated calomel electrode (SCE) was used as the reference electrode and the counter-electrode. The results were

Table 1
Sample preparation conditions and its characteristics

Sample no.	(M/C)/wt.%	X^-	Reduction temperature/°C	$B = h^2 + k^2 + l^2$	a/Å	$10^8 d_{AN}$/m	$S_{AN}/m^2\ g^{-1}$
1	0.5		20	3, 4, 11,...	4.102		
2	0.5	Cl^-	20	3, 8,...	4.104	27.2	0.011
3	0.5	Br^-	20	3, 12,...	4.088	3.54	0.081
4	0.5	I^-	20	3, 8, 11, 12,...	4.096	2.05	0.139

recorded by cyclic voltammetry using a potentiostat (model RDE4 Pine Instruments Company, USA) and a x–y recorder (Type 3086, Yokogawa Hokushin Electric, Tokyo, Japan).

The exact amount of catalyst embedded on the tip of microelectrode was not measured. However, all results measured with SE-ME can be reproduced with an error of 5%, and so the data from different catalysts can be compared without further calibration.

Soft-embedded rotating-disc electrode

To investigate the mechanism of oxygen reduction on a Ag + Darco KB catalyst, a soft-embedded rotating-disc electrode (SE-RDE) with a platinum ring electrode was used as working electrode. The details of making an SE-RDE can be found elsewhere [15]. The collection coefficient of the ring–disc electrode was $N = 0.414$. The rotation speed of the disc electrode was controlled by the HR-101A rotating electrode equipment (Hokuto Denko Ltd., Japan). Potential–current curves were recorded by the potential sweep method at a sweep rate of 5 mV s^{-1}. The potentiostat and x–y recorder were the same as above. The measurement of the amount of catalyst embedded on the SE-RDE was difficult. However, because the data can be repeated within an error of 5%, it can reasonably be assumed that the amount of embedded catalyst was the same in each measurement.

The electrolyte used was a 1.0 M KOH solution made with analytical grade KOH. It was saturated by oxygen gas before testing. All experiments were carried out at a temperature of 30°C maintained by a thermostat. The reference electrode was a SCE and the counter-electrode was a platinum foil.

All potential data reported in this paper are referred to the standard hydrogen electrode (SHE).

Cyclic voltammogram

Cyclic voltammetry was used to check the catalytic activity of the Ag + Darco KB catalyst for hydrogen peroxide reduction in 1.0 M KOH solution. For comparison, the peroxide reduction on "Darco KB" was also measured.

3. Results

3.1. TEM results

Utilizing the oxygen-containing groups present on the carbon surface to prepare metal + support catalyst is a traditional method [16]. In many cases, it is not as efficient as we had hoped. When the Darco KB support was impregnated in $AgNO_3$ solution without any pretreatment, very large Ag particles were obtained; all particles were larger than 100 nm, and some of them were larger than 1 μm (catalyst sample 1).

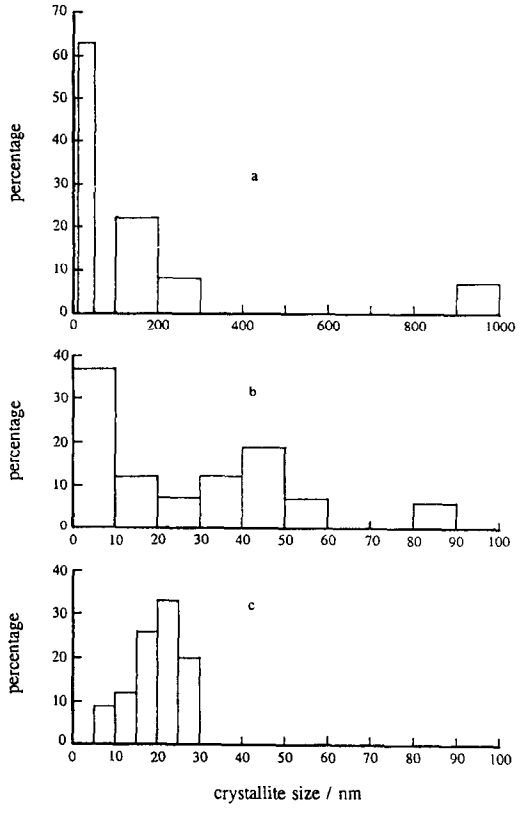

Fig. 1. Particle size distributions of Ag + Darco KB dispersions: (a) sample 2; (b) sample 3; (c) sample 4.

When Darco KB is pretreated by impregnation in a halide solution the Ag particle size dispersion can be varied widely, and if different halide ion preadsorptions are used, the resulting Ag + Darco KB catalyst can have different Ag particle size distributions.

Fig. 1 shows the Ag particle size distributions in samples 2–4 determined by the TEM method. It can be seen that, when carbon is preadsorbed with Cl^-, more than 60% of the Ag particles are smaller than 50 nm. However, a few large particles with diameters greater than 900 nm are still formed. When the functional ion is Br^-, more than 80% of the particles have diameters less than 50 nm. While I^- is preadsorbed on the carbon, all Ag particles are less than 30 nm in diameter and the range of particle size distribution is much narrower than in the previous cases. The sequence of the ability to disperse metal is $I^- > Br^- > Cl^-$.

Before the reducing agent was added to reaction bath, no visible silver halide particles can be seen in TEM with a magnification as high as 300 000. This result suggested that the metal particles were formed from molecular silver halide. After the reduction of Ag(+) from its halide, no signal from halogen element can be detected from the Ag particle by EDS analysis.

The accurate measurement of the Ag particle surface area in these samples was not easy. However, based on the data for particle size distribution, an approximate Ag sur-

face area can still be calculated using a mathematical model such as the following equations based on the square root of the particle diameter:

$$d_{AN} = \sqrt{\sum f_i d_i^2 / \sum f_i} \quad (1)$$

$$S_{AN} = 6W/d_{AN}\rho \quad (2)$$

where d_i is the particle diameter, f_i is the percentage of particles with a diameter d_i, W is the metal loading in the catalyst, ρ is the metal density and S_{AN} is the average surface area. All calculated d_{AN} and S_{AN} data are listed in Table 1.

The crystal structure of Ag particles formed in these different samples was analysed by the SAD method. All Ag particles can give SAD patterns with different signal strengths. The Ag particle crystal lattice parameter can be calculated with the following equations [17]:

$$Rd = \lambda L \quad (3)$$

$$\frac{R_1}{R_2} = \frac{\sqrt{(h_1^2 + k_1^2 + l_1^2)}}{\sqrt{(h_2^2 + k_2^2 + l_2^2)}} \quad (4)$$

$$\frac{1}{d^2} = \frac{h^2 + k^2 + l^2}{a^2} \quad (5)$$

where R is the radius of the diffraction ring in the SAD pattern, d is the lattice plane distance, a is the lattice parameter, $h^2 + k^2 + l^2 = B$ are the Miller indices, λ is the electron wavelength and L is the camera length. In practical use, λL is called the camera constant and can be determined using a standard sample.

All calculated values of a and B are listed in Table 1. The Ag crystal has a face-centred cubic (fcc) structure with a standard lattice parameter $a = 4.077$ Å. From the a data and B data in Table 1, it is apparent that all Ag particles supported on Darco KB have the fcc structure with a lattice parameter slightly larger than the standard value (expansion < 0.7%).

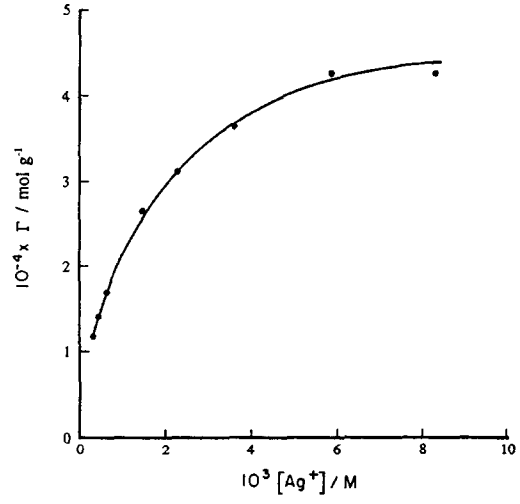

Fig. 2. Adsorption curve of Ag^+ on Darco KB carbon at 20°C.

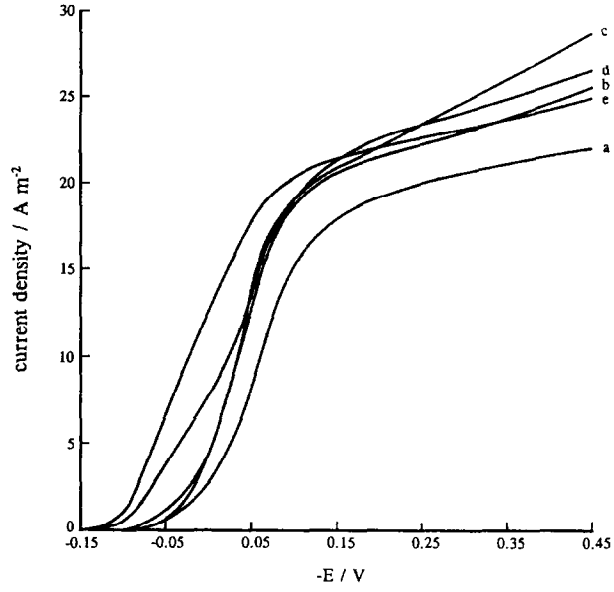

Fig. 3. Cathodic current–potential curves of oxygen reduction in 1.0 M KOH measured at a potential sweep rate of 1 mV s^{-1}: (a) Darco KB; (b) catalyst 1; (c) catalyst 2; (d) catalyst 3; (e) catalyst 4.

3.2. Adsorption result

Ag^+ can be adsorbed on Darco KB activated carbon. Fig. 2 shows the adsorption curve of Ag^+ on Darco KB. For a $AgNO_3$ solution with a Ag^+ concentration of 50 mg l^{-1}, the adsorbance of Ag^+ is about 15 mg g^{-1} Darco KB.

3.3. Electrocatalysis results

Fig. 3 illustrates the polarization curves of oxygen reduction for samples 1–4 and Darco KB supports measured by the SE-ME method. It can be seen that oxygen reduction at Ag + Darco KB has two distinct features. The first is that in the potential region of $E > -0.10$ V, the cathodic current increased with decreasing Ag particle size. In particular, when $E > +0.05$ V, the cathodic current in the carbon support was very low but was increased by factors of 4.8 and 10 in samples 2 and 4 respectively. The second feature is that, when potential was sufficiently negative enough ($E < -0.1$ V) all samples showed approximately the same current; in this potential region, the current increased slowly as the potential became more negative. These results suggest that oxygen reduction on small Ag particles follows a two-electron mechanism.

To confirm this deduction, another test was designed. Fig. 4 shows cyclic voltammograms for the reduction of HO_2^- at Ag + Darco KB and at a Darco KB support. It is apparent that Ag + Darco KB has only a medium catalytic

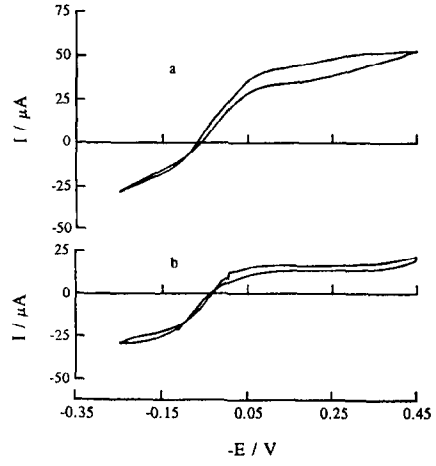

Fig. 4. Cyclic voltammograms at a SE-ME embedded with (a) Ag + Darco KB (sample 4) and (b) Darco KB in 0.01 M H_2O_2 + 1.0 M KOH deaerated with N_2 gas. Potential sweep rate; 2 mV s^{-1}.

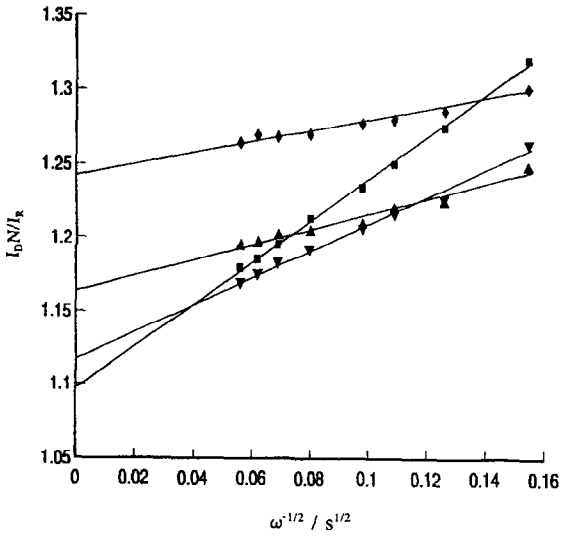

Fig. 6. Plots of I_DN/I_R vs. $\omega^{-1/2}$ for the data in Fig. 5. Disc potential: ♦ −0.25 V; ▲ −0.35 V; ▼ −0.45 V; ■ −0.55 V.

activity for HO_2^- reduction. This result contrasts with those in which Ag was found to be very active for HO_2^- reduction [3].

The oxygen reduction mechanism on Ag is strongly affected by Ag particle size. Fig. 5 shows the potential–current relations of oxygen reduction on sample 1 at several electrode rotation speeds and the intermediate HO_2^- oxidation current measured with an SE-RDE. At a lower rotation speed, the disc current appeared to be limited when $E < -0.2$ V; this is due to the mass transport limitation. At higher rotation speeds, there was a less well-defined limiting current. However, the HO_2^- re-oxidation current is quite high. These results suggest that four- and two-electron reduction of oxygen proceed in parallel. Therefore the ratio of four-electron to two-electron reduction can be calculated as $(I_D/I_R)N$. It was found that this ratio has a linear relation with $\omega^{-1/2}$ where ω is the rotation speed (Fig. 6). The intersection of each line with the vertical axis gives the ratio of four-electron to two-electron reactions without the influence of mass transport at a certain potential. From Fig. 6, it is apparent that this ratio decreases as the potential becomes more negative. Further analysis of this linear relation to determine the kinetic parameters is difficult because the total current

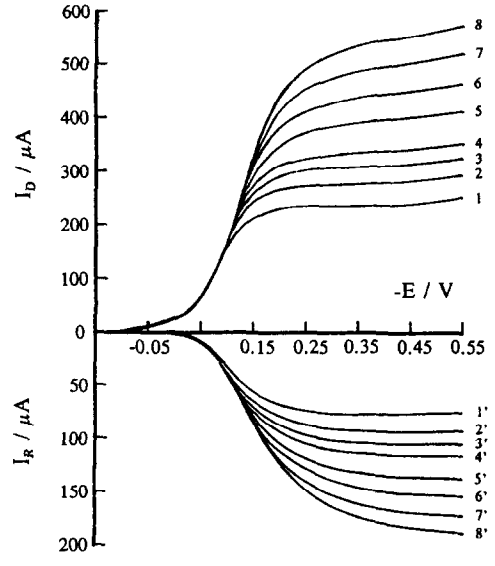

Fig. 5. Polarization curves of O_2 reduction on a sample 1 SE-RDE and of HO_2^- re-oxidation on a Pt ring electrode in 1.0 M KOH saturated with O_2 gas. The Pt ring potential was held at $E = 0.55$ V. The potential sweep rate of the disc electrode was 2 mV s^{-1}. Rotation speed/rev min^{-1}: (1, 1′) 400; (2, 2′) 600; (3, 3′) 800; (4, 4′) 1000; (5, 5′) 1500; (6, 6′) 2000; (7, 7′) 2500; (8, 8′) 3000.

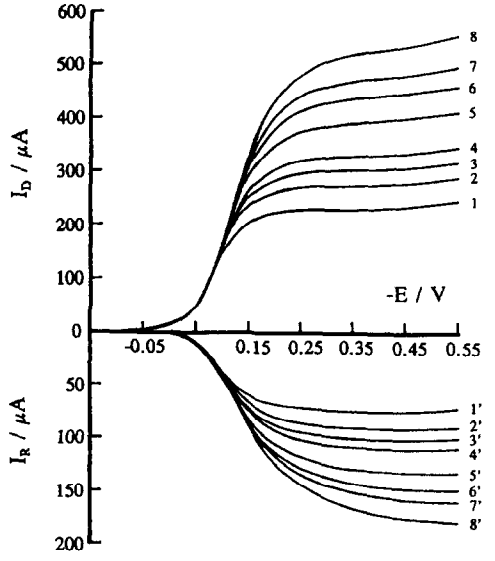

Fig. 7. Polarization curves of O_2 reduction on a sample 4 SE-RDE and of HO_2^- re-oxidation on a Pt ring electrode in 1.0 M KOH saturated with O_2 gas. The Pt ring potential was held at $E = 0.55$ V. The potential sweep rate of the disc electrode was 2 mV s^{-1}. Rotation speed/rev min^{-1}: (1, 1′) 400; (2, 2′) 600; (3, 3′) 800; (4, 4′) 1000; (5, 5′) 1500; (6, 6′) 2000; (7, 7′) 2400; (8, 8′) 3000.

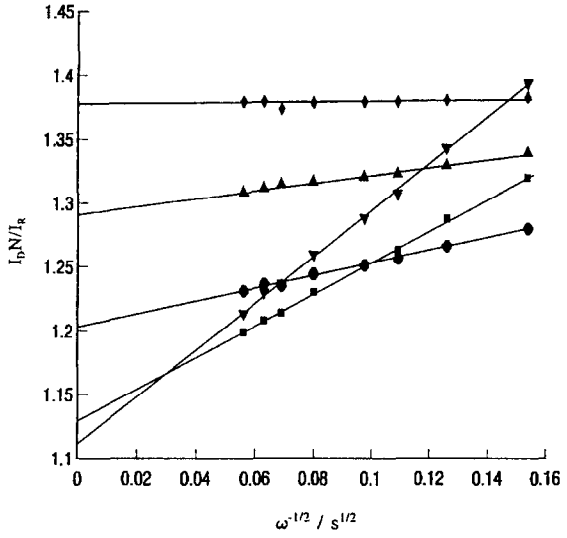

Fig. 8. Plots of $I_D N/I_R$ vs. $\omega^{-1/2}$ for the data in Fig. 7. Disc potential: ◆ −0.20 V; ▲ −0.25 V; ● −0.35 V; ■ −0.45 V; ▼ −0.55 V.

comprises contributions from both silver and the support, and the oxygen reduction mechanisms at these two materials are different. Therefore a suitable model of oxygen reduction on metal + support is needed; several models for single catalyst can be found in the literature [18].

Oxygen reduction at sample 4 was also measured with the SE-RDE. The results are in Fig. 7, and the plots of relative $(I_D/I_R)N$ versus $\omega^{-1/2}$ are shown in Fig. 8. Comparison of Figs. 6 and 8, in the higher-potential region, shows that the four-electron mechanism makes a higher contribution to oxygen reduction on sample 4 than that on sample 1. However, at low potentials the difference between the ratios for the two catalysts becomes smaller.

4. Discussion

The preadsorption of functional ions provides an efficient method of preparing a dispersed metal + support catalyst. The basic principle is similar to that of using the oxygen-containing group present on the carbon support. However, in order for this method to be successful, it is necessary to select a suitable functional ion which will react strongly with the metal precursor. From Fig. 2, it has been calculated that the amount of Ag^+ adsorbed on Darco KB from a $AgNO_3$ solution containing 50 mg Ag^+ l^{-1} is 15 mg g^{-1}. For a catalyst with a Ag loading of 0.5 wt.% (4.6×10^{-6} mol g^{-1}), all Ag^+ is adsorbed on Darco KB and the Ag particles should be fine. However, the particles obtained in practice were still very large, because the interaction between Ag^+ and the carbon support is too weak. The adsorbances of Cl^-, Br^- and I^- on Darco KB were measured as 3.06×10^{-4} mol g^{-1}, 3.76×10^{-4} mol g^{-1} and 4.29×10^{-4} mol g^{-1} respectively [13]. When different halogen ions are selected as the functional ion, all

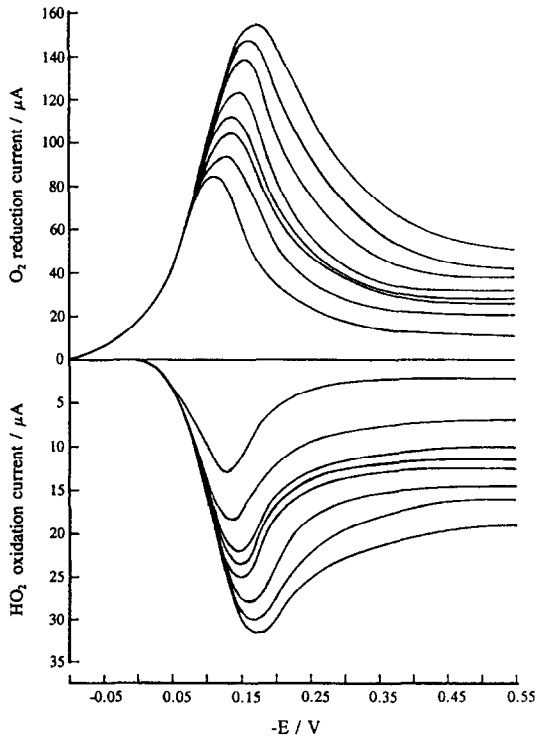

Fig. 9. Polarization curves of O_2 reduction on Ag particle surface (sample 1) and of the intermediate HO_2^- re-oxidation on a Pt ring electrode obtained from Fig. 5.

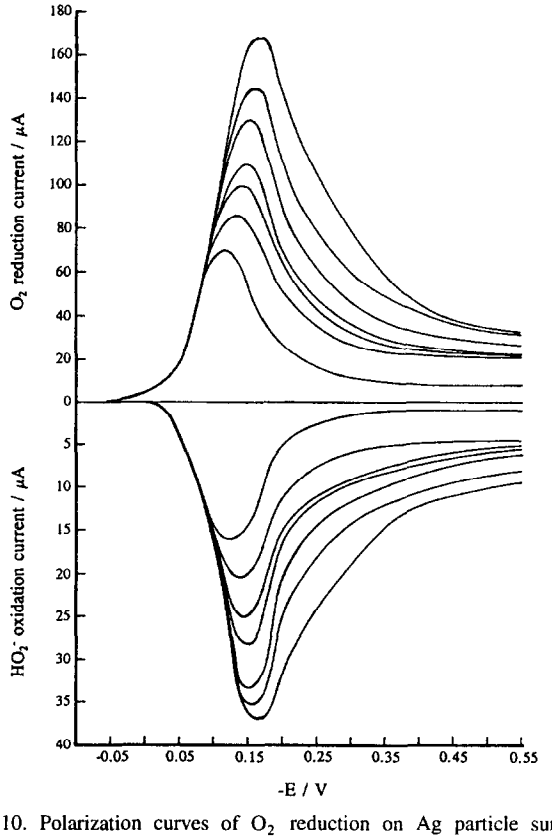

Fig. 10. Polarization curves of O_2 reduction on Ag particle surface (sample 4) and of the intermediate HO_2^- re-oxidation on a Pt ring electrode obtained from Fig. 7.

Ag^+ can be deposited on the support surface with an increased interaction strength, and the Ag particles become smaller. It can be concluded that the strength of the interaction between the metal precursor and the surface functional ions or groups is the main factor controlling the particle size distribution.

To analyse the effects of the metal particle size for oxygen reduction, the first aspect that should be considered is the crystal structure of the metal particle. It is possible that as the particle size decreases, the crystal structure (space lattice) may change. Even when the space lattice does not change, the concentration of various crystallographic sites (crystal faces, edges, corners) may vary with the change in particle size; for example, the surface-averaged distribution of atoms in crystal edges and corners increases with decreasing particle size, but the surface-averaged distribution of atoms in crystal faces decreases with decreasing particle size. According to the TEM data, all Ag particles in samples 1–4 gave a B series of 3, 4, 8, 11, 12,..., although some diffraction spots were too weak to be detected, such as $B = 8$ in sample 1 and $B = 4$ in sample 4. Therefore it can be deduced that all these electron diffraction patterns have [110] zone axes, which means that the crystals are oriented in the electron microscope so that the electron beam is incident on one of the edges of the unit cell. However, the weakened diffraction spots were not the same for different samples. This suggests that the crystal growth has different preferred directions in samples 1–4.

The second complication is the intermediate product of oxygen reduction produced on carbon which can migrate to the metal surface and undergo further reduction at many metal + carbon catalysts. This can give a indirect increase in the four-electron reduction current. It has been shown that the proportion of two-electron reduction for the Ag + Darco KB catalyst is quite high. In addition, Fig. 3 shows that Ag + Darco KB has only a medium activity for HO_2^- reduction. Thus it can be assumed that the contribution of HO_2^- reduction to the total current is not great. Hence, to simplify the discussion, this current could be ignored.

Under these conditions, the discussion of the effects of Ag particle size on oxygen reduction can be simplified because the contribution of oxygen reduction on Ag can be separated from the total on Ag + Darco KB. Figs. 9 and 10 illustrate the current–potential relations of oxygen reduction on Ag particle surface and the related HO_2^- re-oxidation current (the oxygen reduction current at the Darco KB support and the corresponding ring current were subtracted directly from the data in Figs. 5 and 7). A comparison of these two figures shows that the four-electron reduction starts at a more positive potential on large Ag particles than on fine Ag particles, and was much enhanced on smaller Ag particles as the potential became more negative. At very negative potentials ($E < -0.13$ V), the activity of the fine Ag particles for four-electron reduction is higher than that of the large particles.

These results can be explained qualitatively as four-electron and two-electron reductions occur on different active sites: crystal faces for four-electron reduction, and edge and corner sites for two-electron reduction. The activation energy of four-electron reduction on the smaller Ag particles is higher than that on the larger Ag particles. This is the unfavourable effect of Ag particle size on four-electron reduction. However, decreasing particle size results in an increase in metal surface area, and hence an increase in the amount of atoms on the crystal face. This is the favourable effect of Ag particle size for this reaction. The final result is a combination of these two factors.

The HO_2^- re-oxidation current starts at the same potential. This implies that the activation energy was much less affected by the change in Ag particle size. As a result of decreasing particle size (so that the surface-averaged distribution of atoms at the edges and corners increased), the two-electron reduction was enhanced.

Fig. 3 shows that the cathodic oxygen reduction current increased by factors of 4.8 and 10 on samples 2 and 4 respectively, and from Table 1 it can be seen that the corresponding increases in the metal surface areas are 6.4 and 11.6 times.

Based on these results, it can be concluded that oxygen reduction on silver particles is a structure-sensitive reaction.

Another significant result can be deduced from Figs. 9 and 10. Both figures show a peak in both the ring and disc currents in the potential region between -0.12 and -0.18 V. The peak current position shifted towards negative potentials when the rotation speed of electrode increased. This can be explained, as in Ref. 15, in terms of competition between the metal particle and the support surface for oxygen molecules. Because the metal loading is quite low and the surface area of the metal can be ignored compared with that of support, the oxygen reduction rate on the support surface is very low in the potential region $E > -0.15$ V, so the majority of oxygen molecules are reduced on the Ag surface. At very low potentials ($E < -0.15$ V), most of the oxygen molecules are reduced on support surface, further affecting the diffusion layer distribution and resulting in less reactant at the metal surface. This means that, at a highly dispersed metal + support catalyst, the activity of the metal can only be utilized at a higher potential region if the support has a reasonable catalytic activity. The influence of competition is much more serious when the dispersity of the metal is higher.

5. Conclusion

The preadsorption of functional ions is an efficient method for preparing a highly dispersed metal + support catalyst. By suitable selection of the functional ion, this method can be used to produce different metal + support

systems. It can be used for both experimental investigations and practical applications.

Oxygen reduction on Ag particles is a structure-sensitive reaction: four-electron reduction seems to occur at crystal face sites and two-electron reduction at edge and corner sites. The size of the Ag particles affects the different catalytic activity for the four-electron and two-electron reduction of oxygen. The increase in the four-electron reduction current is due to the combination of two factors: the increase in the activation energy and the increase in the amount of atoms on the crystal face as the particle size decreases.

The competition for reactant between the metal and the support surface has a significant influence for the catalytic behaviour of the highly dispersed metal + support catalyst. Therefore the catalytic activity of the metal particle can only be utilized in a potential region where reaction on the support does not occur.

References

[1] E. Yeager, J. Mol. Catal., 38 (1986) 5.
[2] E.L. Littauer and K.C. Tsai, J. Electrochem. Soc., 126 (1979) 1924.
[3] T. Hurlen, Y.L. Sandler and E.A. Pantier, Electrochim. Acta, 11 (1966) 1463.
[4] A. Liebhasfsky and E.J. Cairns, Fuel Cells and Fuel Batteries, Wiley, New York, 1968.
[5] A. Gibney and D. Zuckerbrod in J. Thompson (Ed.), Power Sources, Vol. 9, Academic Press, London, 1983, p. 143.
[6] G.V. Zhutaeva, N.D. Merkulova, I.N. Landau, Z.G. Garakanidze and V.V. Surikov, J. Appl. Chem. USSR, 63(3) (1990) 522.
[7] E.M. Pica and L. Kekedy, Rev. Chim. (Bucharest), 40(11) (1989) 910.
[8] S.D. Seliverstov, N.Y. Lyzlov and Z.P. Arkhangelskaya, J. Appl. Chem. USSR, 57(9) (1984) 1824.
[9] D. Sepa, M. Vojnovic and A. Damjanovic, Electrochim. Acta, 15 (1970) 1355.
[10] G. Bianchi, G. Caprrioglio, F. Mazza and T. Mussini, Electrochim. Acta, 4 (1961) 232.
[11] S.Z. Beer and Y.L. Sandler, J. Electrochem. Soc., 112 (1965) 1133.
[12] P. Fischer and J. Heitbaum, J. Electroanal. Chem., 112 (1980) 231.
[13] Y-F. Yang, Y-H. Zhou, C-S. Cha and W.M. Carroll, Electrochim. Acta, 38(15) (1993) 2333.
[14] J.S. Fritz and G.H. Schenk, Quantitative Analytical Chemistry (4th edn.), Allyn & Bacon, Boston, 1979, p. 209.
[15] Y-F. Yang, Y-H. Zhou and C-S. Cha, Electrochim. Acta, to be published.
[16] P. Ehrburger in A.C. Zettlemoyer and J.T.G. Overbeek (Eds.), Advances in Colloid and Interface Science, Vol. 21, Elsevier, Amsterdam, 1984, p. 275.
[17] B.E.P. Beeston, Electron Diffraction and Optical Diffraction Techniques, North-Holland, Amsterdam, 1972, p. 223.
[18] K. Kinoshita, Electrochemical Oxygen Technology, Wiley, New York, 1992, p. 19.